Computer simulation evidence of the molecular mechanism of makeup removal using cleansing foam
～Is an "in silico formulator" superior to a human formulator?～

Yokoyama, Takahiro[1]; Miwake, Hideki[2]; Hamaguchi, Masugu[3]; Nakatake, Ryouichi[2]; and **Arai, Noriyoshi**[1][*]

[1] Department of Mechanical Engineering, Keio University, 3-14-1 Hiyoshi, Kohoku-ku, Yokohama, Kanagawa 223-8522, Japan;
[2] Research Institute, Fancl Corporation, 12-13 Kamishinano, Totsuka-ku, Yokohama, Kanagawa 244-0806, Japan;
[3] Kirin Central Research Institute, Kirin Holdings, 26-1, Muraoka-Higashi 2-chome. Fujisawa, Kanagawa 251-8555, Japan

＊ Noriyoshi Arai, Department of Mechanical Engineering, Keio University, 3-14-1 Hiyoshi, Kohoku-ku, Yokohama, Kanagawa 223-8522, Japan, +81-45-566-1846, arai@mech.keio.ac.jp

Abstract

Aqueous cleansing agent cosmetics are mainly used to remove oily stains from makeup and are multi-component aqueous solutions consisting of various surfactants, moisturizers, and pH regulators. In the development of cosmetics, experiments are repeated until the desired physical properties are obtained from an enormous number of formulation designs. Here, molecular simulation is a common technique to investigate the molecular behaviors such as self-assembly. Therefore, the use of molecular simulations to visualize phase states that cannot be observed experimentally, and to elucidate the molecular mechanism of cleansing, is expected to be beneficial to the industry. In this study, we investigate the self-assembly structure of a multi-component cleansing-agent system (up to seven components) using a coarse-grained molecular technique. The self-assembly structure varies greatly (vesicle, lamellar, or network), depending on the type and ratio of molecules in the formulation. By evaluating the structures with respect to their potential energy and dispersibility, we investigated the relationship between cleansing performance and self-assembled structure of a formulation. The cleansing performance increases as the self-assembly structure develops from simple to complex higher-order structures. Certain surfactants with weakly hydrophilic groups increase the complexity of the self-assembled

structure, resulting in better cleansing performance. The proposed simulation approach could help reduce the huge cost of iterative trials and identify possible new formulations.

Introduction.

Cleansing foam is used to wash excess sebum and dirt from the skin, while a makeup remover is used, as implied by its name, to remove make-up cosmetics. Recently, in the interest of lessening application time and environmental impact, there is an increasing push toward combining cleansing foam and makeup remover into one product [1].

Solvent-based cleansing agents such as makeup remover oil have excellent removal strength, since oil is the main component, but there remain issues such as high environmental loads and material costs, in addition to the user feeling residual oiliness after a rinse. By contrast, surfactant-type cleansing agents such as cleansing foams have excellent rinsing properties but weak removability, since they are water-based [2]. In this context, we aimed to improve the cleansing performance of cleansing foams. However, cleansing foams are typically composed of many ingredients, making it difficult to find the best formulation from an infinite number of combinations.
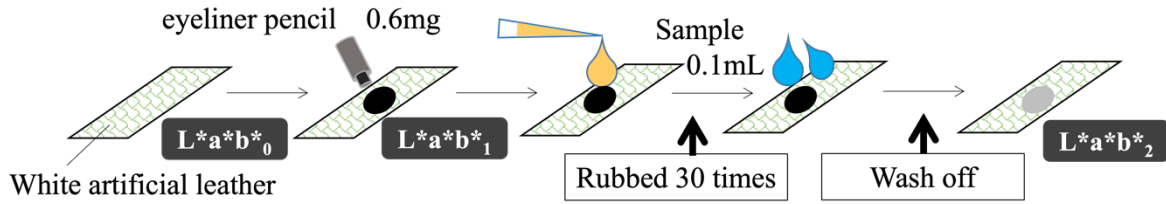
Simulations were used to understand the essential molecular mechanism of the cleansing process. Molecular simulations provide visualizations of the assembly structure [3,4] and the cleansing process at nano spatial-temporal scales, which are difficult to observe experimentally. To clarify the molecular mechanism of cleansing will help reduce the high cost of formulation design; consequently, we performed investigations by reproducing various formulations using molecular simulations and comparing their structures and cleansing capability. Our study presents a guide to manipulating the cleansing performance of multi-surfactant solutions with regard to cosmetics.

Materials and Methods.

1. **Experimental Data.**

    Cleansing foam samples (over 150 formulations) consisting of ionic surfactants, non-ionic surfactants, polyols, and water were prepared by heating while mixing thoroughly by stirring. Some examples of ingredients are listed in Fig. 2. To test the prepared samples, first, a waterproof eyeliner pencil was applied on a piece of white artificial leather, which was dried for 30 min. Then, 0.1 mL of the corresponding cleansing foam sample was added on the dried eyeliner, which was rubbed 30 times, rinsed, and dried. At last, the cleansing capability was evaluated using the eyeliner residue calculated by color differences. A schematic of all procedures is shown in Fig. 1.

Evaluation of cleansing capability

$$\text{Cleansing capability (\%)} = \frac{\sqrt{(L*1-L*2)^2+(a*1-a*2)^2+(b*1-b*2)^2}}{\sqrt{(L*1-L*0)^2+(a*1-a*0)^2+(b*1-b*2)^2}} \times 100$$

L*a*b* value were measured by a colorimeter (CM-2600d, Konica Minolta, Inc.)

Figure 1: Schematic of the evaluation test to determine the cleansing capability of the prepared formulations in this study. L* indicates lightness, a* and b* indicate chromaticity, and L*a*b* is the color space measured by a colorimeter (CM-2600d, Konica Minolta Inc.). $L*a*b*_0$, $L*a*b*_1$, and $L*a*b*_2$ represent the color space value of the white artificial leather before applying the eyeliner, after applying it, and after cleansing it, respectively [5].

2. Simulation Method.

Dissipative particle dynamics (DPD) method [6-8], one of the coarse-grained molecular techniques was used to reproduce the molecular structure of a multi-component system containing various surfactants and polyols. In this method, a group of atoms is coarse-grained as a virtual particle which makes it possible to calculate larger systems, which have been difficult to apply due to computer limitations. DPD method has been applied to a variety of surfactant systems [9,10]. In particular, in recent years DPD has been actively used to study self-assembly in multi-component systems [11,12]. The fundamental equation in DPD method is Newton's equation of motion, and three types of forces: conservative, dissipative, and random are subjected to all DPD beads. Newton's equation of motion for the particle i is given as follows:

$$m_i \frac{dv_i}{dt} = f_i = \sum_{j \neq i} F_{ij}^C + \sum_{j \neq i} F_{ij}^D + \sum_{j \neq i} F_{ij}^R \qquad (2.1)$$

where m is the mass, v is the velocity, F^C is the conservative force acting from other particles, F^D is the dissipative force due to momentum exchange with other particles, and F^R is the random force causing thermal motion of particles. Details of the force formula have been given elsewhere [13]. Note that interactions in the DPD method are related to the solubility parameters. To determine the interaction parameters of the mesoscopic simulation models, we used J-OCTA simulation software [14]. This software estimates the cohesive energy, solubility, the Flory–Huggins parameter, and the equilibrium structures of each molecule.

We adopted a mesoscopic representation of the molecular components of cleansing foams. Since there are literally countless ingredients used in cosmetic products, we modeled typical molecules that are commonly used as shown in Fig. 2. Roughly classified, there are surfactants, polyols and water as solvent. We modeled 36 molecules including 17 surfactants, 17 polyols, citric acid, and water (as a solvent). Polyols are used in cleansing agents as a moisturizer to prevent the skin from drying out, which causes serious damage, and also as foaming enhancers, and as feeling adjusters. Citric acid is a pH adjuster to maintain quality and performance of the product during its shelf time.

Two different series of DPD simulations for over 150 formulations were carried out in this study. In each formulation, the molecules species included and their ratios differ. From

random initial configuration, simulations were conducted in constant-volume and constant-temperature ensembles until the system would reach equilibrated. The first series is for reproducing the self-assembled morphology itself of a super multi-component system in aqueous solution. Thus, a periodic boundary condition is adopted for all directions of the simulation cells. The second series is for reproducing the morphology when the cleansing agents are applied to the dirty surface. This system is sandwiched with hydrophobic walls at the top and bottom of the simulation cells. The inner surface of a hydrophobic wall is treated as smooth wall. The force field of the smooth wall is derived on the basis of a structured wall by summing the DPD forces between every pair and wall bead. Details of the force formula of smooth wall have also been given elsewhere [15]. To model the wall as an oil-based stain, we set the potential of the wall to equal that of a pure alkyl chain.
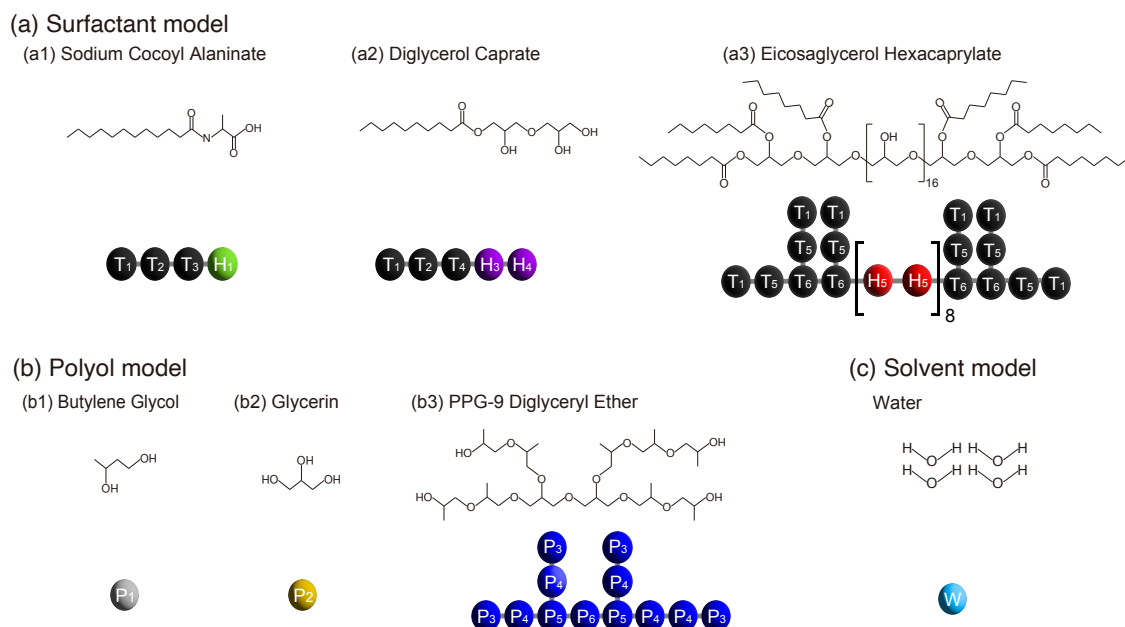

Figure 2: Molecular structure and mesoscopic coarse-grained models of representative (a)surfactants, (b)polyols, and (c)water. The hydrophobic beads are depicted in black, and hydrophilic beads are depicted in various colors.

Results and Discussion.

1. Self-assembed morphology.

We conducted course-grained molecular simulations for over 150 formulations in order to reproduce the molecular structures of multi-component systems containing various surfactants and polyols. Each system consisted of, at most, 7 different components at various ratios. As a result, many self-assembled morphologies were obtained depending on the formulation as shown in Fig. 3 sorted by cleansing capability γ obtained from experiments. It is a well-known fact that amphiphilic molecules construct supramolecular structures based on hydrophobic interaction, such as surfactants form vesicles or lamellar structures in aqueous solutions [16]. Our simulation results also showed that surfactants constract various self-assembled structures through the hydrophobic tail beads (black) keeping away from water while the hydrophilic head beads (other colors) coming in contact with water. In the same way, mixed lamellar structures (Fig. 3a3) and mixed vesicles (Fig. 3a4) are simply formed. In other cases, however, weakly hydrophilic head groups assembled in the center of rod-like vesicles (Fig. 3b4) or in the central layer of a lamellar structure (Fig. 3c3) without coming into contact with water, despite being the hydrophilic head groups of a surfactant. In the studied systems, which deals with a lot of components, the degree of interaction varies, even among the hydrophilic groups. Thus, the weakly hydrophilic groups become energetically stable by being incorporated inside self-assembled structures in contact with other hydrophilic groups, but not with water. This is the reason certain molecules with weakly hydrophilic groups such as eicosaglycerol hexacaprylate (EH, Fig. 2a3) are captured inside the aggregates (Fig. 3b2-4, 3c1-4).

The self-assembled structures are formed due to the amphiphilic nature of molecules. On the other hand, small polyols like butylene glycol (BG, Fig. 2b1) or glycerin(Fig. 2b2) behave differently in a multi-component system. On the scale we are dealing with, BG and glycerin cannot be coarse-grained into hydrophobic and hydrophilic parts, which means it is regarded as a hydrophilic particle overall. Therefore, some particles are incorporated inside the aggregate structures and are contact with hydrophilic head groups or attached to the surfaces of the aggregates near water, while the rest are dissolved in water (Fig. 3a1, b4, c4).

Other polyols, such as PPG-9 diglyceryl ether (PPG9-DE, Fig. 2b3) also showed different behavior compare to that of the surfactants and small polyols. Depending on the formulation,

the polyols are sometimes incorporated into the interior of aggregates (Fig. 3c3) and sometimes appear on the surface of structures (Fig. 3c1). This is due to the fact that amphihilic nature of polyols is weaker comapred to surfactant since polyols don't contain pure alkyl chains. Because of the strength of the hydrophobic interaction of polyol particles is not strong, their energetically stable position in the structure depends on the formulation.

When we compare those self-assembled structures of cleansing foams with their cleansing capability γ, it is highly expected that there is a certain correlation between them. As shown in Fig. 3, the self-assembled structures of cleansing foams with low γ are simple rod-like micelles, vesicles, and double bi-layers while those with high γ were more complex, such as multi-layers, and network structures. This result implies the importance of linking the performance of a cleansing foam with its self-assembled morphology to better understant the molecular mechanism of high-performance cleansing foams.
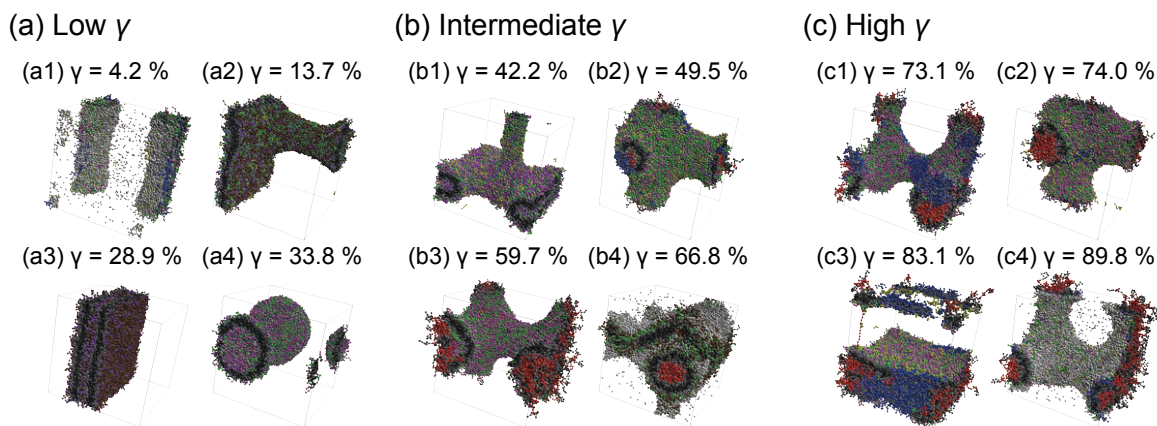

Figure 3: Representative snapshots of equilibrium morphologeis of cleansing foams with (a) low, (b) intermediate, and (c) high cleansing capability γ. Water beads are eliminated for clarity.

2. Correlations between structures and cleansing capability.

To quantitatively link the cleansing performances with the morphologies of assembled structures, the potential enery U, contact area of the structure/water interface S, and dispersion B_2 were calculated for the equilibrium structures of all formulations. Potential energy of a system was calculated by integrating the coservation forces for all interactions. For the value S, by counting the number of particles which have water particles within certain distance, we considered that value to be equivalent to the surface area. We set the certain distance same as cutoff distance. Dispersion B_2 is obtained through integrating radial distribution function (RDF) between particles [17,18]. Fig. 4 shows the relation between S and B_2 of all structures obtained from simulations. It can be observed that S and B_2 have a strong positive correlation. Both values are low when the structures are organized into a small condensed aggregate, such as rod-like micelles, vesicles, or bi-layers. These values tend to be higher when the number of layers of a lamellar structure increases, or the rod-like vesicles assembled from various directions and formed a network structure. Using these indexes, we were able to grasp the change of structures shifting from vesicles or bi-layers to multi-layers or network structures quantitatively.
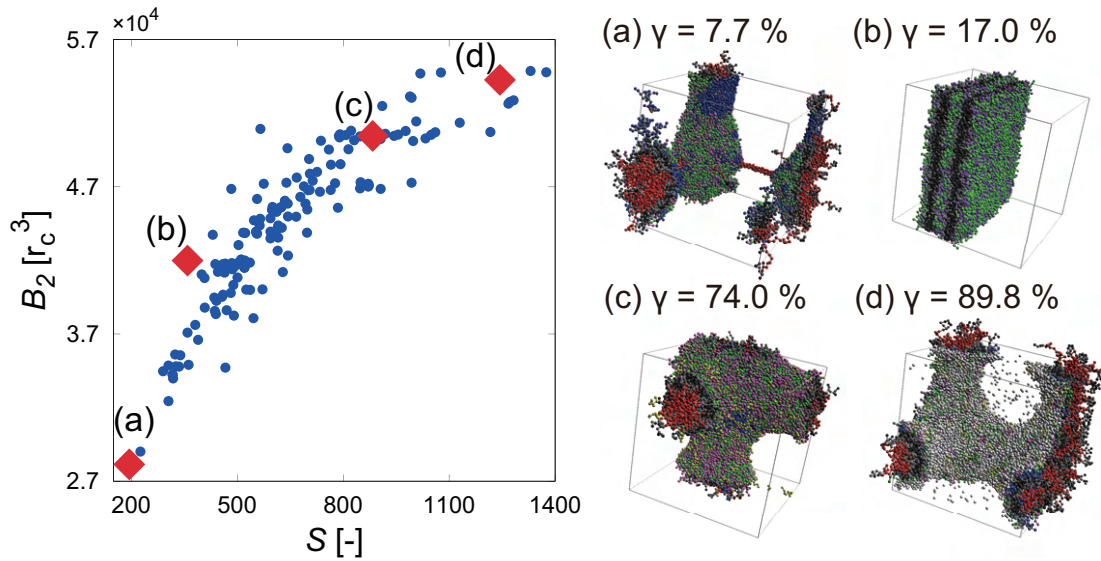

Figure 4: Correlation between dispersion B_2 and contact area of the structure/water interface S. (a-d) Representative snapshots of the self-assembled structures when B_2 and S are (a) low, (b) moderately low, (c) moderately high, and (d) high.

We calculated those values which represent the entire aggregates and compared them to the cleansing ability obtained from experiments. For S, we counted all particles which are close to water, and for B_2, we calculated RDF between all kinds of particles except water to obtain the information of the entire structure. The scatter diagrams in Fig. 5 show the relationship between the cleansing capability γ as a function of the values for the entire structure. The correlation coefficients between the values and γ were calculated. When compared to γ, U has correlation coefficients above 0.4, while S and B_2, which represent aggregate shapes, have lower correlation coefficients (0.3~0.4). These positive correlations indicate that the more complex the self-assembled structure of the cleansing agent components, the higher the performance. Nevertheless, the calculated correlation coefficients (0.3-0.4) are low, indicating that the correlations are not strong enough to conclude that the cleansing performance depends only on the self-assembled structures. Therefore, it is likely that there are other factors affect the performance.
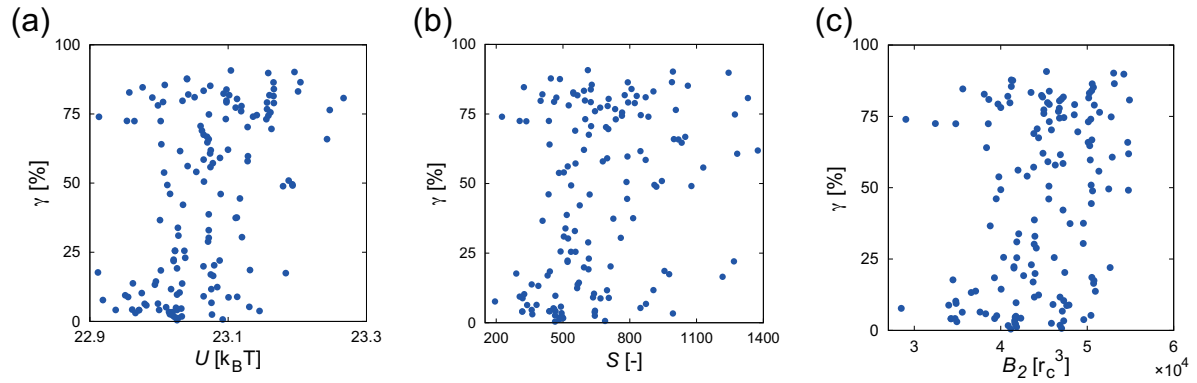

Figure 5: Scatter diagrams of the correlations between cleansing capability γ and simulation values which represent the aggregate state and structure: (a) potential energy U of entire system, (b) contact area of the structure/water interface S, and (c) dispersion B_2 of all particles except water.

Further detailed analyses of the formulations were conducted, such as the distribution of specific particles and molecules. Firstly, we discovered that specific molecules which make self-assembled structures comlex by being incorporate inside the aggregates such as EH are playing important role to realize effective cleansing agents. We calculated the value of B_2 for EH to compare to γ. In Fig. 6, we show the relationships between γ and B_2 of EH and also γ and mole fraction of EH to clarify that the behaviors inside the aqeous solution are crucial to macroscopic properties. As in Fig. 6, B_2 of EH has a strong positive correlation with γ while mole fraction of EH doesn't show a clear correlation. The correlation coefficients are 0.52 and 0.27 respectively. Thus, it should be noted that simply adding large amounts of EH won't necessarily ensure good cleansing performance; EH must be well dispersed. When EH is included in a system with other surfactants with strongly hydrophilic parts, such as several hydroxyl, carboxy, or sulfo groups, EH will avoid being in contact with water. Thus, other surfactants will cover both the hydrophobic groups and EH, which induces complex structures in aqueous solution. As a result, a multi-layer aggregate will form with a hydrophobic layer, hydrophilic layer, and EH layer as shown in Fig. 3b2-4, 3c1-4.
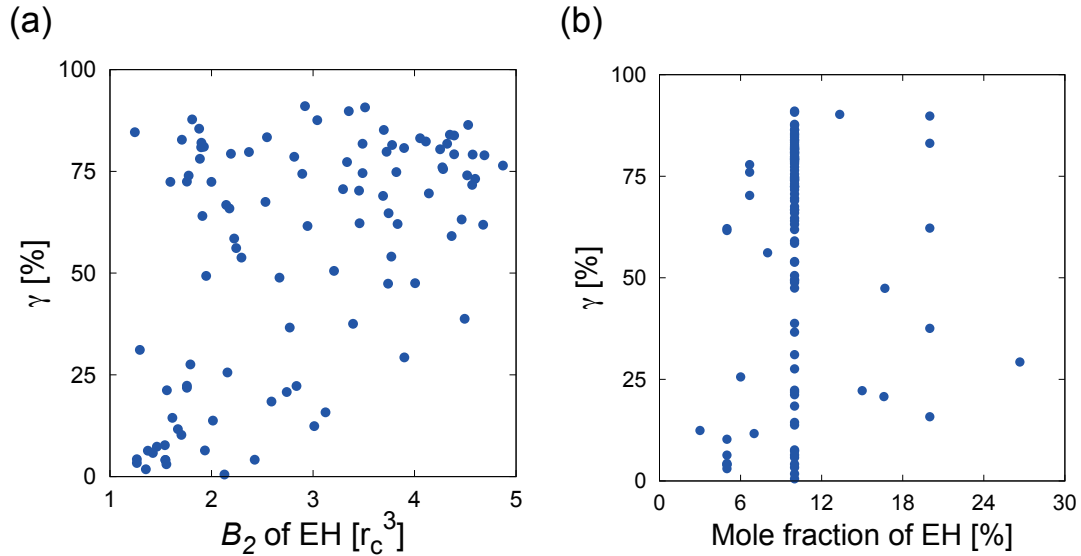

Figure 6: The correlations between cleansing capability γ and (a) dispersion B_2 of EH, and (b) mole fraction of EH respectively.

Subsequently, we focus on the hydrophobic (HO) particles which are the trigger of cleansing process by adsorbing to surface of oil-based stain. We considered the HO particles which are made of pure alkyl chains and do not include ester bond, amido bond, or ether bond in them. In the same way as the analysis of EH, we calculated the dispersion B_2 of HO particles inside the aggregates and compared them to cleansing capability γ. Fig. 7(a) shows the relationship between γ and B_2 of HO particles, and it is suggested that they have negative correlation. The correlation coefficient was -0.4, which means the lower the dispersion of HO particles, the higher the cleansing performance. Hence, cleansing agents become effective when the HO particles are well condensed. We also show the relationship between γ and mole fraction of HO particles in Fig. 7(b). Although there is no clear correlation, it was observed that γ tends to be lower when the mole fraction of HO particles is higher than a moderate amount. This suggest that the excessive amount of HO particles may cause a bad effect to cleansing process.
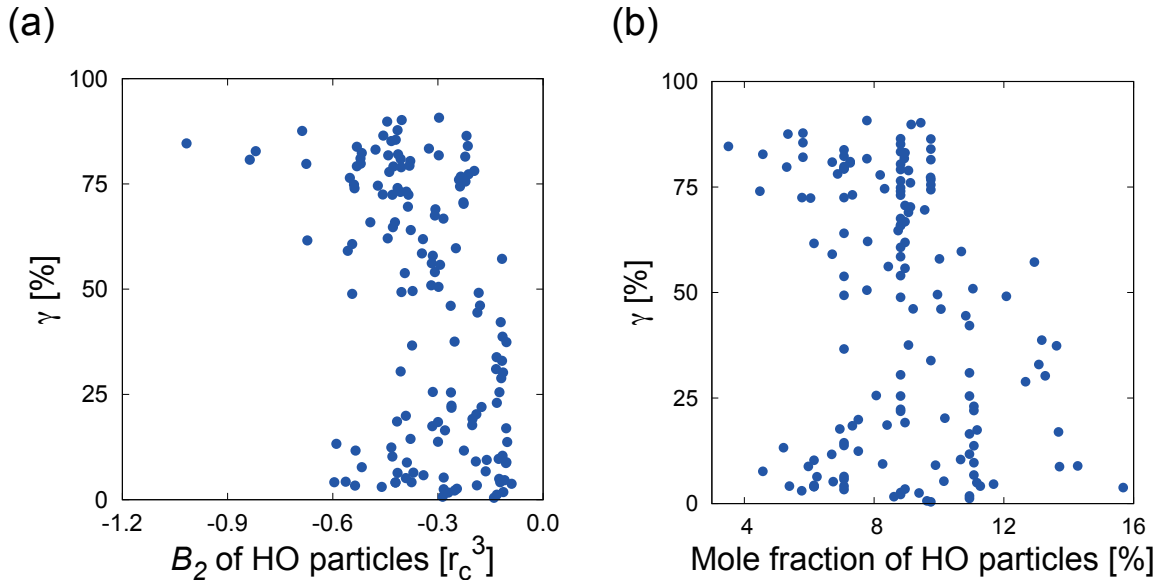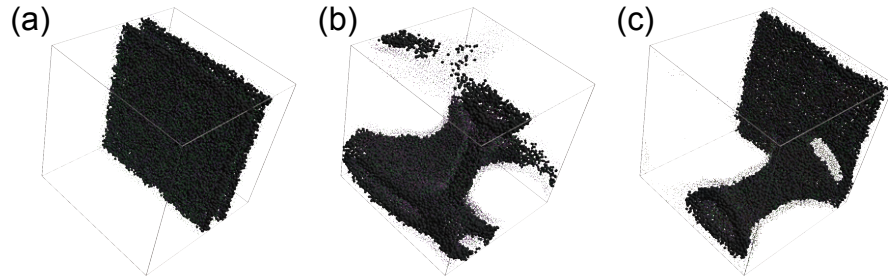
(a)

(b)

Figure 7: The correlations between cleansing capability γ and (a) dispersion B_2 of HO particles, and (b) mole fraction of OH particles respectively.

To observe the behaviors of HO particles, the representative snapshots of equilibrium morphologies are shown in Fig. 8, where the HO particles (black) are exaggerated by making other particles smaller. For the structures with high dispersion of HO particles, HO particles exist throughout the entire self-assembled structures, while for those with low dispersion of HO particles, they exist only in a part of the self-assembled structures. Despite Fig. 8[a], [d] show the same lamellar structures, the distributions of HO particles are different. In Fig. 8 [a], HO particles exist in the entire layers, while in Fig. 8[d], there are some spaces composed of other than HO particles. Based on these, it is suggested that adding excessive amounts of HO particles would result in the presence of HO particles throughout the self-assembled structures, which would reduce the performance.

From these analyses, it can be suggested that not only the entire self-assembled structures, but also the particles constituting the self-assembled structures and their distributions contribute to the cleansing performance of cleansing agents.

High Dispersion of HO Partiles

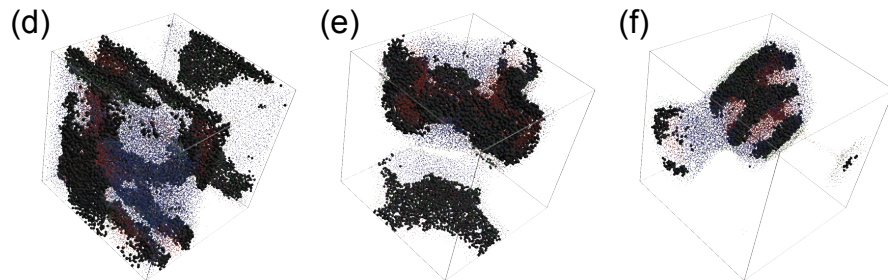

Low Dispersion of HO Partiles

Figure 8: Representative snapshots of equilibrium morphologeis of cleansing foams with (a-c) high, (d-e) low B_2 of HO particles. Here HO particles are shown in balck and other particles are depicted small. Water beads are eliminated for clarity.

3. Self-assembled morphologies between hydrophobic slit.

For further investigation of the self-assembled structures of cleansing agents, we conducted another series of DPD simulations by placing the coarse-grained models of cleansing agents between a hydrophobic slit which can be regarded as oil-based stains. We reproduced the same formulations of cleansing agents as in Section 1 between the hydrophobic slit. We chose the potential of the smooth wall of the hydrophobic slit same as the most-hydrophobic particle containing pure alkyl chains. The representative equilibrium structures of this system are shown in Fig. 9. Various layered structures are obtained depending on the formulations, but the HO particles being adsorbed on the surface of the hydrophobic slit wall were common for all formulations. The inner distribution of each aggregate is also the same as that of the system shown in Section 1 without the hydrophobic slit. These equilibrium morphologies represent the state of the cleansing agent ingredients adsorbed on oil-based stains, before they were removed.
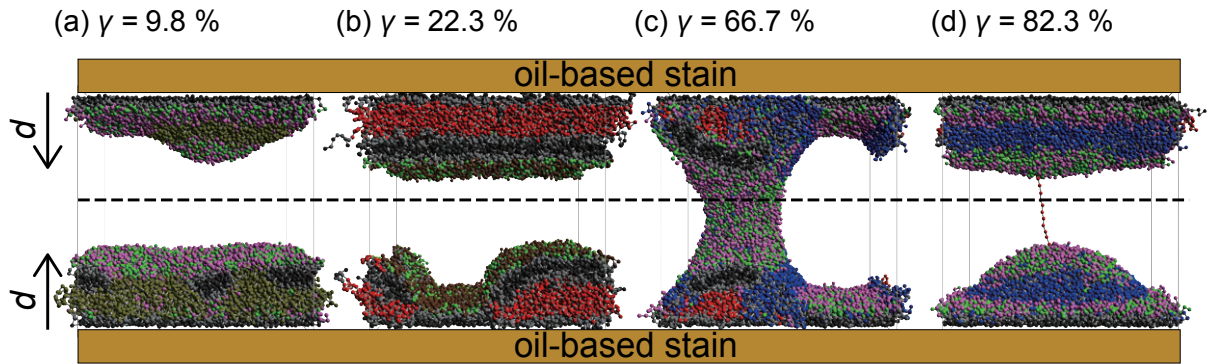

Figure 9: Representative snapshots of equilibrium morphologies of cleansing foams between a hydrophobic slit with (a) low, (b) moderately low, (c) moderately high, and (d) high cleansing capability γ. Water beads are eliminated for clarity.

To analyze this system, we calculated the density distribution ρ of HO particles (ρ_{HO}) as a function of distance d from the hydrophobic walls. Fig. 10 shows the $\rho_{HO}(d)$ for all simulations with coloring the high performance system to be blue, and low performance to be orange. The heights of the second peak of $\rho_{HO}(d)$ are higher for the formulations with low γ. When the hydrophobic particles in the second layer create a flattened layer structure (Fig. 9a, b), it is inferred that the mobilities of surfactants are restricted, which will negatively affect the cleaning process. Hence, the addition of excessive quantity of HO particles may cause a bad effect to realize an effective cleansing.
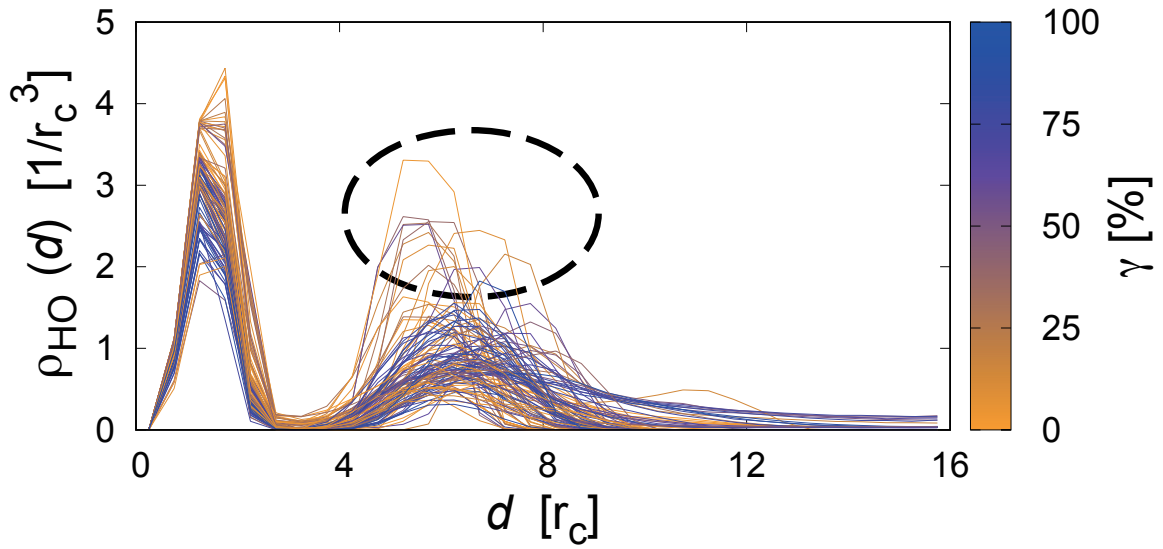

Figure 10: Density profiles of hydrophobic particles as a function of distance d from the hydrophobic wall for all formulations. The color indicates the cleansing capability γ of the formulation.

Conclusion.

We investigated the mechanism of cleansing by simulating the self-assembled structures of multi-component systems considered as cleansing agents. For reproducing the self-assembled morphology, we adopted coarse-grained models of some representative surfactants and polyols which are often used in products. Based on the DPD simulations, various self-assembled structures such as vesicles, rod-like vesicles, bi-layers, and network structures are obtained depend on the formulations. Through evaluating those structures using values such as potential energy, surface area, and dispersion, the relationship between cleansing capabilities and self-assembled structures can be directly compared.

It was quantitatively shown that the entire self-assembly structures formed inside the aqueous solution were linked to the cleansing capability. As a result, we learned that the complexity of a structure is one of the features of high-performance cleansing agents. However, the correlation between the performance of cleansing agents and their entire self-assembled structures are not strong enough.

Thus, more detailed analyses are conducted to investigate the inner distribution of aggregates. As a result, we discovered that a certain molecule plays an important role in cleansing process. In particular, EH is a crucial key to realize a high-performance cleansing foam. Since this surfactant contains a weakly hydrophobic head groups compared to carboxy, or sulfo groups, it is incorporated inside the aggregate and make the structure complex. This non-ionic surfactant leads to effective cleansing process through being dipersed throighout the structure. Thus, it should be noted that simply adding EH is not effective but the dispersion of EH is.

We also discovered that hydrophobic particles which play an important role in the first step of cleansing, are important to be effective. In detail, when the dispersion of HO particles inside the aggregates are low, the cleansing capability becomes higher. On the other hand, by adding excessive amounts of HO particles, those particles will be well dispersed throughout the aggregate, and this state is not good for the performance of cleansing foams. This can be also shown through the second series of DPD simulation between hydrophobic slits. The analysis of density profile of HO particles showed that when the HO particles are concentrated in the second layer from the dirty surface, the cleansing ability is low. The flat second layer composed of HO particles is energetically

stable. Thus, it is suggested that the mobilities of surfactants are restricted which results in poor performance of the cleansing process.

These findings indicate the potential for establishing novel in-silico formulations with good cleansing performance, which will greatly simplify and reduce the cost of developing formulations compared to iterative experimental trials.

Conflict of Interest Statement. NONE.

References.

1. K. Watanabe, N. Sakurai, T. Meno, C. Yasuda, S. Takahashi, A. Hori, K. Tsuchiya and K. Sakai. Novel Spontaneous Cleansing Feature of Foam ─Hybrid Bicontinuous-Microemulsion-Type Foamy Makeup Remover ─. *Journal of Society of Cosmetic Chemists of Japan*, vol. 55, pp. 19–27, 2021.

2. K. Watanabe, M. Masuda, K. Nakamura, T. Inaba, A. Noda, T. Yanagida and T. Yanaki. A new makeup remover prepared with a system comprising dual continuous channels (bicontinuous phase) of silicone oil and water. *IFSCC Magazine*, vol .7, pp. 310–318, 2004.

3. R. Goetz and R. Lipowsky. Computer simulations of bilayer membranes: Self-assembly and interfacial tension. *J. Chem. Phys.*, vol. 108, pp. 7397-7409, 1998.

4. A. Sarkar, R. Sasmal, C. Empereur-mot, D. Bochicchio, S. V. K. Kompella, K. Sharma, S. Dhiman, B. Sundaram, S. S. Agasti, G. M. Pavan and S. J. George. Self-Sorted, Random, and Block Supramolecular Copolymers via Sequence Controlled, Multicomponent Self-Assembly. *J. Am. Chem. Soc.,* vol. 142, pp. 7606 ─ 7617, 2020.

5. T. Iwanaga, K. Uchida, N. Takeuchi and Y. Abe. Development of Oil-Type Make-up Remover Prepared with Polyglycerol Fatty Acid Esters. *Journal of Society of Cosmetic Chemists of Japan*, vol. 39, pp. 186–194, 2005.

6. Y. Kong, C. W. Manke, W. G. Madden and A. G. Schlijper. Simulation of a confined polymer in solution using the dissipative particle dynamics method. *Int. J. Thermophys.*,Vol. 15, pp. 1093-1101, 1994.

7. A. G. Schlijper, P. J. Hoogerbrugge and C. W. Manke. Computer simulation of

dilute polymer solutions with the dissipative particle dynamics method. *J. Rheol*., Vol. 39, pp. 567-579, 1995.

8. P. Hoogerbrugge and J. Koelman. Simulating microscopic hydrodynamic phenomena with dissipative particle dynamics. Europhys. Lett., Vol. 19, pp. 155–160, 1992.

9. R. L. Anderson, D. J. Bray, A. D. Regno, M. A. Seaton, A. S. Ferrante and P. B. Warren. Micelle Formation in Alkyl Sulfate Surfactants Using Dissipative Particle Dynamics. *J. Chem. Theory Comput*., Vol. 14, pp. 2633 − 264, 2018.

10. M. Choudhary, and S. M. Kamil. Phase Diagram Study of Sodium Dodecyl Sulfate Using Dissipative Particle Dynamics. *ACS Omega*, Vol. 5, pp. 22891-22900, 2020.

11. K. P. Santo and A. V. Neimark. Dissipative particle dynamics simulations in colloid and Interface science: a review. *Adv. Colloid Interface Sci.*, Vol. 298, p. 102545, 2021.

12. A. Vishnyakov, R. Mao, K. Kam, A. Potanin and A. V. Neimark. Interactions of Crosslinked Polyacrylic Acid Polyelectrolyte Gels with Nonionic and Ionic Surfactants. *J. Phys. Chem. B*, Vol. 125, pp. 13817-13828, 2021.

13. N. Arai, Y. Yoshimoto, K. Yasuoka and T. Ebisuzaki. Self-assembly behaviours of primitive and modern lipid membrane solutions: a coarse-grained molecular simulation study. *Phys.Chem.Chem.Phys.*, Vol. 18, pp. 19426-19432, 2016.

14. J-OCTA, JSOL Corporation, https://www.jsol-cae.com/product/material/jocta/, j-octa.

15. N. Arai, K. Yasuoka and X. C. Zeng. Self-Assembly of Triblock Janus Nanoparticle in Nanotube. *J. Chem. Theory Comput*., Vol. 9, pp. 179-187, 2013.

16. V. P. Torchilin. Structure and design of polymeric surfactant-based drug delivery systems. *J. Control. Release*, Vol. 73, pp. 137-172, 2001

17. T. Inokuchi, K. Moroboshi, and N. Arai. Multiscale prediction of functional self-assembled materials using machine learning: high-performance surfactant molecules. *Nanoscale*, Vol. 10, pp. 16013-16021 , 2018.

18. J. Liu, Y. Gao, D. Gao, L. Zhang and Z. Guo. Nanoparticle Dispersion and Aggregation in Polymer Nanocomposites: Insights from Molecular Dynamics Simulation. *Langmuir*, Vol. 27, pp. 7926-7933, 2011